Pressure-induced phase transition of B-type Y_2O_3*

Qian Zhang(张倩)[1,†], Xiang Wu(巫翔)[2], and Shan Qin(秦善)[3]

[1] *Gemological Institute, China University of Geosciences, Wuhan* 430074, *China*
[2] *State Key Laboratory of Geological Processes and Mineral Resources, China University of Geosciences, Wuhan* 430074, *China*
[3] *Key Laboratory of Orogenic Belts and Crustal Evolution, Ministry of Education & School of Earth and Space Sciences, Peking University, Beijing* 100871, *China*

(Received 3 May 2017; revised manuscript received 15 May 2017; published online 18 July 2017)

The synthesized monoclinic (B-type) phase of Y_2O_3 has been investigated by *in situ* angle-dispersive x-ray diffraction in a diamond anvil cell up to 44 GPa at room temperature. A phase transition occurs from monoclinic (B-type) to hexagonal (A-type) phase at 23.5 GPa and these two phases coexist even at the highest pressure. Parameters of isothermal equation of state are $V_0 = 69.0(1)$ Å^3, $K_0 = 159(3)$ GPa, $K_0' = 4$ (fixed) for the B-type phase and $V_0 = 67.8(2)$ Å^3, $K_0 = 156(3)$ GPa, $K_0' = 4$ (fixed) for the A-type phase. The structural anisotropy increases with increasing pressure for both phases.

Keywords: Y_2O_3, x-ray diffraction, pressure-induced phase transition, equation of state

PACS: 07.35.+k, 61.05.cp, 91.60.Hg **DOI:** 10.1088/1674-1056/26/9/090703

1. Introduction

Sesquioxides are very important materials which possess a wide range of physical and chemical properties and can be used for different technological applications. For example, they play a vital role in the grain growth inhibitor,[1] are used as additives of ceramics[2] and active catalysts for organic reactions,[3,4] and have potential use in nuclear engineering.[5,6] In addition, sesquioxides can adopt perovskite (Pv), post-perovskite (PPv), and post-PPv phases at extreme conditions, which has significant implications for the mantle of giant extrasolar silicate planets. For instance, Al_2O_3 undergoes a series of pressure-induced phase transitions from corundum structure to Rh_2O_3(II)-type structure, then to the PPv-type structure, and finally to the post-PPv phase (U_2S_3-type, *Pnma* and $Z = 4$) above 370 GPa.[7] Gd_2S_3-type (*Pnma* and $Z = 4$) and Th_2S_3-type (*Pnma* and $Z = 4$) structures, which have the same space group and cationic coordination numbers with the U_2S_3-type structure, have been observed in Sc_2O_3[8] and Ti_2O_3[9] at high pressure, respectively.

The high-pressure behavior of rare-earth sesquioxides has been widely investigated. So far, five polymorphic forms have been identified in rare-earth sesquioxides. Hexagonal A ($P\bar{3}m1$) in which cations are in seven-fold coordination, monoclinic B ($C2/m$) in which cations are mixed with six or seven-fold coordination, and cubic C ($Ia\bar{3}$) with six-coordinated cations are commonly observed at room temperature and ambient pressure.[10] The two other phases denominated as H (hexagonal, $P6_3/mmc$) and X (cubic, $Im\bar{3}m$) are formed at high temperature.[11] Cations in Gd_2S_3, Th_2S_3, and U_2S_3 occupy seven and eight oxygen coordinations, which are higher than those in C, B, A, Pv, and PPv structures.

Scandium and yttrium elements with the chemically similar lanthanide elements are often known to belong to the lanthanide family as the rare-earth metal elements. The optical properties of trivalent rare earth ion-doped nanocrystalline materials have been investigated extensively. Y_2O_3 nanocrystals doped with trivalent rare earth ion have attracted considerable interest because of the high chemical durability and thermal stability. Eu-doped Y_2O_3 is an important commercial luminescent material, it has been widely used in fluorescent lamps, projection television tubes, field emission displays, etc.[12] Y_2O_3 crystallized into the C-type structure under ambient conditions. Lots of attempts have been made to understand its high-pressure behavior, but the high-pressure phase transition sequences show some inconsistencies. As for the pure Y_2O_3, the C→B,[13,14] C→B→A,[15–17] C→A,[18] and C→B→Gd_2S_3[19,20] phase sequences have been observed in experiments or theoretical calculations. The *in situ* high-pressure luminescence spectra indicated that the C-type bulk Eu-doped Y_2O_3 transformed into the B-type phase at 15 GPa, while 20 nm-sized nanocrystals did not.[21]

As we all know, the experimental results are influenced by experimental conditions, such as non-hydrostaticity of pressure and regime of temperature treatment. In the static high-pressure experiment at 2.5 GPa and 1273 K, the C-type Y_2O_3 transformed to the B-type phase which was also found above 12 GPa in a shock-compression experiment, while the A-type phase was proposed to be the favorable stable high-pressure phase.[14] In some quasi-hydrostatic compression experiments at room temperature, Y_2O_3 followed the phase sequence of C→B→A.[15–17] A high-pressure Raman experiment reported two phase transitions, viz, C→B and B→A

*Project supported by the National Natural Science Foundation of China (Grant Nos. U1232204 and 41502029) and China Postdoctoral Science Foundation (Grant No. 2015M580679).

†Corresponding author. E-mail: qianzhang@cug.edu.cn

© 2017 Chinese Physical Society and IOP Publishing Ltd

at 12 GPa and 19 GPa respectively.[16] However, a high-pressure x-ray experiment showed that pure Y_2O_3 exhibited a direct transition to A structure at 12.1 GPa and room temperature, whereas the C→B→A transition was observed in Eu-doped Y_2O_3.[18] Considering the temperature effect, a sequence of structural phase transitions C→B→A observed in the room-temperature compression did not coincide with the phase transition sequence C→B→Gd_2S_3 under high pressure and high temperature.[19] Moreover, there are some inconsistencies among the room-temperature data collected with different internal pressure standards under conditions close to hydrostatic environment by noble gases like He or Ne media and by solid or liquid media such as KBr and silicone oil.[22] The previous pressure-transmitting media in the experiments on Y_2O_3 were silicone oil,[18] a mixture of methanol and ethanol,[23] or KBr powder.[16]

To the best of our knowledge, starting Y_2O_3 samples used in the former work were characterized by the C-type structure. The B-type polycrystalline Y_2O_3 has been synthesized successfully using multi-anvil press in our previous work.[24] High-pressure x-ray diffraction experiments provide us information about high-pressure phase transitions and physical properties.[25–27] In this study, we carry out the high-pressure experiment of B-type Y_2O_3 as the starting material up to 44 GPa by *in situ* x-ray diffraction (XRD) in diamond anvil cell (DAC).

2. Experiment

The starting sample of the synthesized B-type Y_2O_3 was described in detail in Ref. [24]. In our XRD experiment, we generated high pressures by a symmetric type DAC with 300 μm-diameter culets. A 150 μm-diameter hole was drilled in the pre-indented to ∼ 30 μm-thickness rhenium gasket. Pt was loaded in the chamber as pressure standard based on its well-known equation of state.[22] and Ne was used as the pressure medium. The *in situ* high-pressure XRD experiment at room temperature was conducted at 13IDD at Advanced Photon Source (APS). Diffraction patterns were collected using a MarCCD detector. The monochromatic x-ray which was focused to 5 μm×5 μm on the sample surface has a wavelength of 0.3344 Å. Collection time for each pattern was 20 s. Diffraction images were integrated to one-dimensional spectra using the Fit2D program.[28] Lattice parameters were obtained using Unitcell.[29] Some x-ray diffraction patterns were fitted by the Le Bail method implemented in the GSAS+EXPGUI software.[30]

3. Results and discussion

The XRD pattern at ambient conditions gives lattice parameters $a = 13.892(7)$ Å, $b = 3.494(1)$ Å, $c = 8.614(4)$ Å, $\beta = 100.22(4)$, and $V = 411.4(2)$ Å^3 from a full profile model refinement. *In situ* high-pressure XRD data were collected up to 44 GPa at room temperature. Some selected XRD patterns are shown in Fig. 1, where all peaks can be indexed into the B-type Y_2O_3 and minor impurities up to 23.5 GPa. All peaks shifted to higher angles of 2θ with increasing pressure. As shown in Fig. 1, the peaks began to change at 23.5 GPa, indicating the appearance of a new phase. According to the previous studies,[19] the new phase would be either A- or Gd_2S_3-type. By performing the x-ray profile fitting analyses and comparing the d values of the characteristic peaks with the previous experimental data,[19] we confirmed that the new phase adopted the A-type structure ($P\bar{3}m1$). Upon compression, the B-type phase was found to obviously coexist throughout the transition process from the B- to A-type phase. The B-type phase still existed at the highest pressure, implying that the transition may be kinetically sluggish. In Sc_2O_3, the B to A transition at 77 GPa was predicted by *ab initio* calculation,[31] but the Gd_2S_3-type phase as the post-B phase was observed above 18 GPa at the high temperature experiment.[8] Considering the similarity of Sc_2O_3 and Y_2O_3, Sc_2O_3 would also have the C→B→A phase transition sequence in the high-pressure experiment at room temperature. As previously mentioned, it is not a common phenomenon that the high-pressure structure sequence of Y_2O_3 observed in the room temperature compression does not coincide with the phase transition sequence at high temperature. Generally speaking, the temperature effect is always considered in pressure-induced phase-transition experiments in order to obtain clear high-pressure structural information, because high temperature relaxes the differential stress and overcomes the potential kinetic effects on phase transition. Therefore, the laser heating usually promotes the phase transition to happen at lower pressure than that of the room temperature compression experiment. By analyzing the crystal structures of B- and A-type phases of Y_2O_3 at high pressure, the B-type structure was found to be equivalent to the A-type structure.[19] This is a possible reason why the B to A transition was observed under compression at room temperature. In our synthesis experiment, we tried to synthesize the Gd_2S_3-type phase of Y_2O_3 in a multi-anvil apparatus at HP-HT conditions (20 GPa and 1800 °C), but the B-type phase was reserved.[24] Ovsyannikov *et al*. tried to obtain the B-type Sc_2O_3 at 14 GPa and 1600 °C, but only the C-type phase was found in the recovered sample.[32] These results show that the HP-HT behaviors of Y_2O_3 and Sc_2O_3 are complex and further investigations of their P–T phase diagrams are needed.

The B- and A-type unit-cell volumes showed a smooth decrease with the increasing pressure. The unit-cell volume data as a function of pressure is plotted in Fig. 2 and analyzed by the second-order Birch–Murnaghan equation of state (B–M EoS).[33] The EoS parameters we obtained are listed in Table 1, which also includes the available experimental and theoretical data for comparison. The equilibrium volume V_0

obtained from the theoretical computation is underestimated compared with the experimental results, which is typical for the LDA computations. The isothermal bulk moduli of B- and A-type Y_2O_3 compounds are approximate. Our result is consistent with the theoretical simulation data,[11] which shows that the difference between the bulk moduli of B- and A-type rare-earth sesquioxides is considerably small.

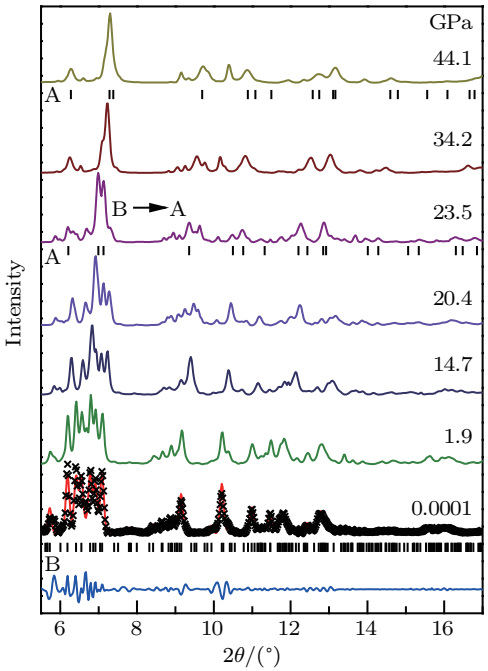


Fig. 1. (color online) X-ray diffraction profiles of the Y_2O_3 sample under room temperature compression. The tick marks indicate the calculated positions of the diffraction peaks of B- and A-type phases with the LeBail method (GSAS). Solid line, symbols, and solid line at the bottom represent the calculated and the observed patterns and their differences at ambient conditions, respectively. Other solid lines represent the observed patterns at high pressure.

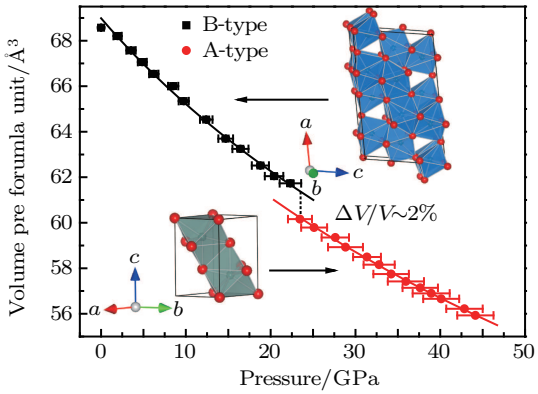


Fig. 2. (color online) The volume per formula of B- and A-type phases of Y_2O_3 as a function of pressure. The solid lines correspond to the second-order B–M EoS fitting to the experimental data. The volume collapse in the phase transition is about 2% at 23.5 GPa. The crystal structures are also shown. Red spheres are oxygen and dark green spheres at the center of polyhedra are yttrium.

The phase transition from B- to A-type Y_2O_3 is followed by a volume collapse of 2% at 23.5 GPa (Fig. 2), which is at the same level as that of Sm_2O_3.[34] This transformation involves only a slight deformation. Compared to this B→A transition, the C→B first-order phase transition is accompanied by a more significant volume decrease (8%,[16] 12.5%[15]).

Table 1. Equation of state parameters for the B- and A-type polymorphs of Y_2O_3. V_0, B_0, and B_0' are the volume per formula unit, the bulk modulus, and its pressure derivative at zero pressure, respectively.

Y_2O_3	V_0/Å^3	B_0/GPa	B_0'	Method
B-type	68.99(10)	159(3)	4 (fixed)	XRD (this study)
	68.55(12)	155(4)	4 (fixed)	XRD[19]
	66.16	117.9	4.83	DFT-LDA[19]
	71.42	192(10)	4 (fixed)	XRD[15]
A-type	67.79(17)	156(3)	4 (fixed)	XRD (this study)
	66.78(53)	159(15)	4 (fixed)	XRD[19]
	64.63	144.6	4.37	DFT-LDA[19]

The coordination number of Y increases from six or seven in B-type structure, to seven in the A-type one during the B→A transition. In addition, the B ($C2/m$) and A ($P\bar{3}m1$) have a group-subgroup relationship.[35] Contrary to the C→B reconstructive transition, the B→A transition is inferred to be displacive, which is also suggested in other studies.[17,19]

Theoretical analysis of pressure-induced B to A-type phase transitions shows a linear correlation between bulk modulus, transition pressures, and the ionic radius of the cation.[11] The suggested transition pressure and bulk modulus for Y_2O_3 are at the same level as those of our experimental results. The difference is mainly due to the GGA exchange correlation energy, which gives a larger V_0 and a smaller B_0. The first single-crystal study of Sc_2O_3 exhibited that the denser B-type phase is a bit more compressible than the C-type one.[32] This result did not confirm the other experimental studies on powdery Sc_2O_3.[8] The previous studies on powders of lanthanide sesquioxides did not reveal a noticeable difference in the bulk moduli of C-, B-, and A-type phases, e.g., Ho_2O_3 and Sm_2O_3.[34,36] Whether there exist noticeable bulk modulus differences among the C-, B-, and A-type rare-earth sesquioxides requires more experimental and theoretical investigations.

During the past few decades, the rare-earth sesquioxides have been studied by numerous researchers to investigate the phase relationships among the C, B, and A phases. Early in 1966, Hoekstra found that the effect of ionic radius is much greater than temperature or pressure in shifting the C↔B equilibrium line.[37] Moreover, compression experiments and theoretical results exhibited that higher pressure would be needed to stabilize the A-type phase in rare-earth sesquioxides with smaller cationic radius.[11,34] However, this systematics of the C→B→A phase sequence may not be applicable to the rare-earth sesquioxides only according to their cationic radii. The comparative crystallography in rare-earth sesquioxides has been summarized in other study.[8] Sc_2O_3 (Sc^{3+}; 0.745 Å),

In_2O_3 (In^{3+}; 0.800 Å), and Y_2O_3 (Y^{3+}; 0.900 Å), which adopt the C-type structure at ambient conditions, crystallize into the Gd_2S_3 structure at high pressure after laser heating.[8,19,38] It is possible that the Gd_2S_3 structure would be found as a post B-type structure in other rare-earth sesquioxides at high temperature.

The pressure evolution of the lattice parameters of the B- and A-type phases is shown in Fig. 3. Regarding the unit-cell compressibilities, the *a* axis is the most compressible and the *b* axis is the least compressible for the B-type phase. As for the A-type Y_2O_3, the *c* axis is more compressible than the *a* axis mainly because of the large intervals between the layers in the *c* axial orientation. It indicates that the axial compressiblities of B- and A-type phases are anisotropic.

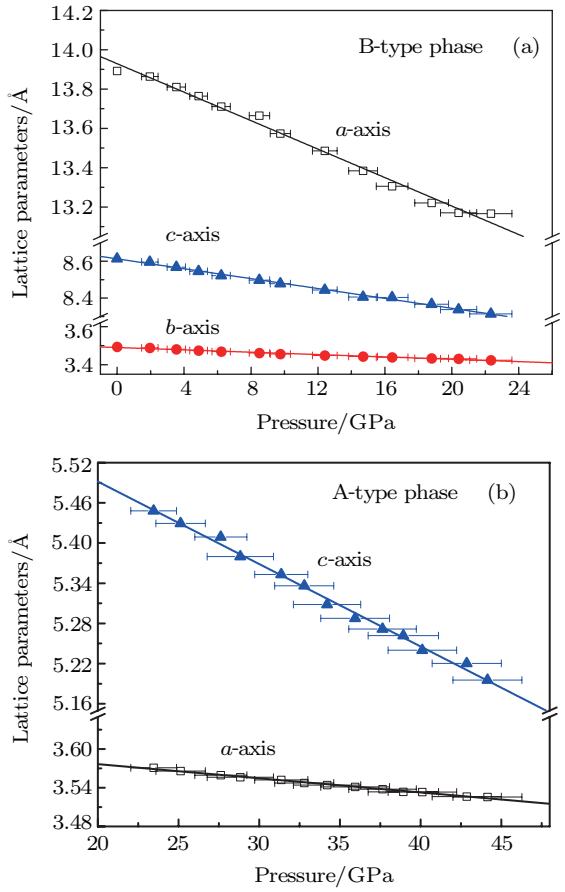


Fig. 3. (color online) Pressure-induced variations in the lattice parameters of the B-type (a) and A-type (b) phases of Y_2O_3. The solid lines are linear fittings of the experimental data.

4. Conclusion

The structural properties of B-type Y_2O_3 under compression have been investigated by synchrotron radiation x-ray diffraction experiment with neon as the pressure-transmitting medium at room temperature up to 44 GPa. We observed a sluggish phase transition from B- to A-type phase at 23.5 GPa. The isothermal *P*–*V* relationship of Y_2O_3 was described by the second-order Birch–Murnaghan equation of state with $B_0 =$ 159(3) GPa for the B-type phase, and 156(3) GPa for the A-type phase. Note that the high pressure behavior of rare-earth sesquioxides is apparently complex, and there are lots of unanswered questions in their condensed matter physics. Further studies will bring exciting results on their high-pressure properties.

Acknowledgements

The authors are deeply grateful to Sergey V. Ovsyannikov and Leonid S. Dubrovinsky for synthesizing the sample. High-pressure experiments were performed at GeoSoil EnviroCARS of the APS, ANL. GeoSoil EnviroCARS operations are supported by the National Science Foundation-Earth Sciences (EAR-1128799) and the Department of Energy Geosciences (DE-FG02-94ER14466). APS is supported by DOE-BES, under Contract No. DE-AC02-06CH11357.

References

[1] Aktas B, Tekeli S and Kucuktuvek M 2014 *Int. J. Mater. Res.* **105** 208
[2] Scott H 1975 *J. Mater. Sci.* **10** 1527
[3] Hussein G A 1996 *J. Anal. Appl. Pyrolysis* **37** 111
[4] Dedov A, Loktev A, Moiseev I, Aboukais A, Lamonier J F and Filimonov I 2003 *Applied Catalysis A: General* **245** 209
[5] Shikama T, Toh K, Nagata S, Tsuchiya B, Yamauchi M, Nishitani T, Suzuki T, Okamoto K and Kubo N 2006 *Nucl. Fusion* **46** 46
[6] Weber W J, Ewing R C, Catlow C R A, de la Rubia T D, Hobbs L W, Kinoshita C, Matzke H, Motta A T, Nastasi M, Salje E K H, Vance E R and Zinkle S J 1998 *J. Mater. Res.* **13** 1434
[7] Umemoto K and Wentzcovitch R M 2008 *Proc. Natl. Acad. Sci. USA* **105** 6526
[8] Yusa H, Tsuchiya T, Sata N and Ohishi Y 2009 *Inorg. Chem.* **48** 7537
[9] Nishio-Hamane D, Katagiri M, Niwa K, Sano-Furukawa A, Okada T and Yagi T 2009 *High Press. Res.* **29** 379
[10] Zinkevich M 2007 *Prog. Mater. Sci.* **52** 597
[11] Wu B, Zinkevich M, Aldinger F, Wen D and Chen L 2007 *J. Solid State Chem.* **180** 3280
[12] Wang H, Uehara M, Nakamura H, Miyazaki M and Maeda H 2005 *Adv. Mater.* **17** 2506
[13] Hoekstra H R and Gingerich K A 1964 *Science* **146** 1163
[14] Atou T, Kusaba K, Fukuoka K, Kikuchi M and Syono Y 1990 *J. Solid State Chem.* **89** 378
[15] Halevy I, Carmon R, Winterrose M L, Yeheskel O, Tiferet E and Ghose S 2010 *J. Phys. Conf. Ser.* **215** 012003
[16] Husson E, Proust C, Gillet P and Itie J 1999 *Mater. Res. Bull.* **34** 2085
[17] Bose P P, Gupta M, Mittal R, Rols S, Achary S, Tyagi A and Chaplot S 2011 *Phys. Rev. B* **84** 094301
[18] Wang L, Pan Y, Ding Y, Yang W, Mao W L, Sinogeikin S V, Meng Y, Shen G and Mao H 2009 *Appl. Phys. Lett.* **94** 061921
[19] Yusa H, Tsuchiya T, Sata N and Ohishi Y 2010 *Inorg. Chem.* **49** 4478
[20] Umemoto K and Wentzcovitch R M 2011 *Phys. Chem. Miner.* **38** 387
[21] Bai X, Song H, Liu B, Hou Y, Pan G and Ren X 2008 *J. Nanosci. Nanotechnol.* **8** 1404
[22] Fei Y, Ricolleau A, Frank M, Mibe K, Shen G and Prakapenka V 2007 *Proc. Natl. Acad. Sci. USA* **104** 9182
[23] Zhang J, Cui H, Zhu P, Ma C, Wu X, Zhu H, Ma Y and Cui Q 2014 *J. Appl. Phys.* **115** 023502
[24] Zhang Q, Wu X, Ovsyannikov S V, Dong J, Qin S, Dubrovinsky L S and Chen D 2016 *Chem. Res. Chin. Univ.* **32** 545
[25] Tang S X, Zhu H Y, Jiang J R, Wu X X, Dong Y X, Zhang J, Yang D P and Cui Q L 2015 *Chin. Phys. B* **24** 096101
[26] Li N N, Li Y, Li H, Tang R L, Zhao Y S, Han D D, Ma Y M, Cui Q L, Zhu P W and Wang X 2014 *Chin. Phys. B* **23** 069101

[27] Yang S W, Peng F, Li W T, Hu Q W, Yan X Z, Lei L, Li X D and He D W 2016 *Chin. Phys. B* **25** 076101
[28] Hammersley A, Svensson S, Hanfland M, Fitch A and Hausermann D 1996 *High Press. Res.* **14** 235
[29] Holland T and Redfern S 1997 *Mineral. Mag.* **61** 65
[30] Toby B H 2001 *J. Appl. Crystallogr.* **34** 210
[31] Liu D, Lei W, Li Y, Ma Y, Hao J, Chen X, Jin Y, Yu S and Cui Q 2009 *Inorg. Chem.* **48** 8251
[32] Ovsyannikov S V, Bykova E, Bykov M, Wenz M D, Pakhomova A S, Glazyrin K, Liermann H P and Dubrovinsky L 2015 *J. Appl. Phys.* **118** 165901
[33] Birch F 1952 *J. Geophys. Res.* **57** 227
[34] Jiang S, Liu J, Lin C, Li X and Li Y 2013 *J. Appl. Phys.* **113** 113502
[35] Hahn T 2002 International Table for Crystallography, A (5th edn.) (Dordrecht: Kluwer) pp. 540, 541
[36] Jiang S, Liu J, Li X, Bai L, Xiao W, Zhang Y, Lin C, Li Y and Tang L 2011 *J. Appl. Phys.* **110** 013526
[37] Hoekstra H R 1966 *Inorg. Chem.* **5** 754
[38] Yusa H, Tsuchiya T, Tsuchiya J, Sata N and Ohishi Y 2008 *Phys. Rev. B* **78** 092107